A generalized multi-scale approach for the design of novel ultra-high-performance concrete

A.Arora[a], B. Mobasher[b], N.Neithalath[b]

a – Post-doctoral Research Scholar, School of Sustainable Engineering and the Built Environment, Arizona State University, Tempe, AZ
b – Professor, School of Sustainable Engineering and the Built Environment, Arizona State University, Tempe, AZ

ABSTRACT

This paper presents a novel strategy to design the binder phase of ultra-high performance concrete (UHPC) from commonly available cement replacement (fly ash, slag, microsilica, metakaolin) and fine filler (limestone) materials. A packing algorithm is used to extract the number density, mean centroidal distance, and coordination number of the microstructure. Similarly, rheological studies on the pastes provide yield stress, plastic viscosity, and mini-slump spread. The selection criteria involves using the three microstructural and three rheological parameters individually or in combination to define packing and flow coefficients. The selection criteria is flexible enough to allow users modify the constraints depending on the application. The binder with the desired packing and rheological features is combined with aggregate sizes and amounts chosen from a compressible packing model based on maximum packing density. A fiber volume fraction of 1% is also used, along with accommodations for wall and loosening effects. The model is programmed in a user-friendly environment to enable engineers select aggregates from locally available materials. Compressive strengths greater than 150 MPa are obtained for the selected UHPC mixtures after 28 days of moist curing. The strength-normalized cost of such mixtures is only a fraction of that of proprietary UHPCs.

Keywords: Ultra High-Performance Concrete; Microstructure; Rheology; Particle Packing; Compressive Strength; Durability

1. INTRODUCTION

Ultra-high performance concrete (UHPC) is an emerging cement-based material with high compressive and tensile strengths, ductility, and long-term durability (B. Graybeal 2011; Russell and Graybeal 2013; Wang et al. 2012; Wille and Boisvert-Cotulio 2015). Some of the applications for which UHPC is well suited for are bridge piers, decks and deck-level connections between modular precast components, blast protection elements, and tunnels (B. A. Graybeal 2012; Maya and Graybeal 2017; Tazarv and Saiidi 2015; Vítek, Coufal, and Čítek 2013). Compressive strengths in excess of 120-150 MPa are generally reported for UHPC mixtures (Yoo and Banthia 2016; B. Graybeal 2011), aided by careful selection of cementitious materials considering their particle sizes and reactivity, and a low water-to-powder ratio, w/p ($0.15 < w/b < 0.23$) to ensure a dense microstructure (Reda, Shrive, and Gillott 1999). The use of non-standard cement replacement materials such as quartz (silica) flour, rice husk ash, and nanoparticles (nanosilica, nano-metakaolin) to achieve high strengths, in additional to common high-performance replacement materials such as silica fume and metakaolin, has been reported (Muhd Norhasri et al. 2016; Ghafari et al. 2015; Z. Li, Venkata, and Rangaraju 2015; Shafieifar, Farzad, and Azizinamini 2017; H. Huang et al. 2017; Ghafari et al. 2014; Van Tuan et al. 2011). Higher strength and durability are direct consequences of microstructure densification, while the use of discontinuous steel fibers (generally greater than 3% by volume) provides sustained post-cracking strengths and ductility (Le Hoang and Fehling 2017).

The material design of UHPC binders is governed by an efficient particle packing process since the low w/p in these mixtures will result in sub-optimal levels of hydration of cement. High material costs and energy implications of UHPC can partly be attributed to the use of large amounts of cement that acts as an expensive filler. It is therefore well accepted that improved packing of the binder phase through the use of cement replacement materials and fine fillers is a better means of strength enhancement than increasing cement content.

This paper implements a multi-scale design strategy to design UHPC mixtures by coupling the design of paste phase at the microstructure level and the aggregate phase at the mesostructure level. This proposed method relies on the premise that, for low w/b concretes where only a fraction of the cement hydrates, (i) improved packing through the use of cement replacement materials and fine fillers is a better means of strength enhancement than increasing cement content, and (ii) better rheology helps better dispersion of the grains, aiding in mixture placement as well as hydration in the presence of low amounts of water, and consequently better mechanical properties.

The design for the optimum aggregate gradation is based on the compressible packing model (De Larrard 1999; Roquier 2016), Contrary to many UHPC mixtures that contain only fine aggregates, the material design reported in this paper considers coarse aggregates (passing 9.5 mm sieve) also. The mechanical strengths and durability performance of the designed UHPC mixtures are also reported. The methodology is designed in such a manner to be implemented in a computer program to optimize the UHPC mixtures from both the performance and cost perspectives.

2. MATERIALS AND METHODS

2.1 Materials

Figure 1 and Table 1 show the physical and chemical properties of the powders used in this study. The water-to-powder ratios (w/p) varied between 0.165 and 0.20 depending on the starting materials used. A polycarboxylate ether (PCE)-based superplasticizer was used. The ratio of solids content of the superplasticizer to the binder content was maintained between 1% and 2%.

Table 1. Chemical composition of the starting materials used for the binders in this study

Components of the binder	SiO_2	Al_2O_3	Fe_2O_3	CaO	MgO	SO_3	LOI
OPC	19.60	4.09	3.39	63.21	3.37	3.17	2.54
Slag (S)	39.41	8.49	0.37	35.53	12.05	2.83	1.31
Fly Ash (F)	58.40	23.80	4.19	7.32	1.11	3.04	2.13

Metakaolin (K)	51.70	43.20	0.50	-	-	-	0.16
Micro silica (M)	> 90.0	-	-	< 1.0	-	-	-
Limestone (L), 1.5 µm	> 97% $CaCO_3$						
Limestone (L), 3 µm							

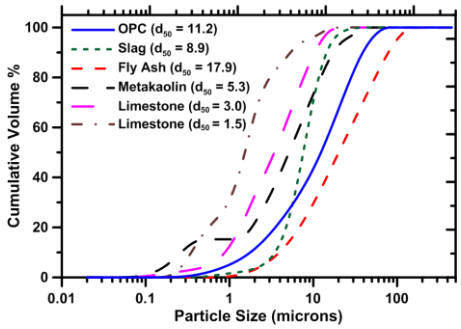

Figure 1. Particle size distribution curves for cement, fly ash, slag, metakaolin, and limestone powders. The median size in microns is shown in parentheses.

The aggregates were classified into three nominal maximum sizes: ¼" (6.25 mm), #4 (4.75 mm), and #8 (2.36 mm). The bulk specific gravity and absorption of the aggregates were determined as 2.65 g/cc and 0.94% respectively. Coarse and fine silica sands were used as fine aggregates, which had median sizes of 0.6 mm and 0.2 mm respectively. The mortar mixtures had both sand types in equal amounts. The mortar cubes and the cylindrical concrete specimens were proportioned using a paste volume fraction of 65%. The fiber reinforced UHPCs employed straight high-strength steel microfibers having a length of 13 mm and a diameter of 0.5 mm.

2.2 Mixing Procedure and Test Methods

All dry powders were thoroughly mixed prior to wet mixing. Paste mixing was performed in accordance with ASTM C 1738 using a M7000 high speed shear mixer. Concrete was mixed in a a mixing bucket made of HDPE. A 12.5 mm Dewalt^{TM} spade drill attached to a spiral drill bit was used as the mixing tool for better shearing of particles. The mixing procedures are detailed in (Arora et al. 2018). The rheological characteristics of all the pastes were determined using TA instruments AR 2000EX rotational rheometer with a vane in cup geometry. The compressive strength of 50 mm mortar cubes was determined in accordance with ASTM C 109 and that of the 75 mm x 150 mm cylindrical concrete specimens in accordance with ASTM C 39.

3. STRATEGIES FOR DESIGNING THE IDEAL PASTE PHASE

Binary, ternary and quaternary blends were proportioned by mixing different amounts of these replacement materials with OPC. The total cement replacement level generally varied between 20 and 30% by mass of OPC. Fly ash or slag were the primary cement replacement materials in ternary and quaternary blends because of their abundance and the larger OPC replacement levels that can be accomplished. Limits to the amounts of micro silica and metakaolin were necessary to ensure adequate dispersion of these materials within the paste. Limestone powders of two different median sizes, either individually, or in equal parts, were used to supplement the binary and ternary mixtures with even finer sizes that they were deficient in, to enhance particle packing.

Table 2 shows the proportions of all the 33 different mixtures (one UHP-control, one HP-control, and 31 UHP pastes) evaluated in the initial phase of this work. All the ultra-high performance (UHP) pastes were proportioned using a volumetric water-to-powder ratio, $(w/p)_v$, of 0.63 (corresponding to a mass-based $(w/p)_m$ of 0.20; 0.22 when the water in the HRWR is also added). In addition to the control UHP paste ($(w/p)_m$ of 0.20), a high performance OPC paste with a $(w/p)_m$ of 0.32 was also proportioned. A commercially available high range water reducer (HRWR) was used at

a solids content of 1.25% by mass of the powder to improve the workability. In Table 2, UHP-control refers to the control mixture made using OPC alone and a $(w/c)_m$ of 0.20, and HP-control refers to the mixture made using a $(w/c)_m$ of 0.32.The HRWR dosage for the HP-control mixture was 2% by mass of the powder. From a large matrix of paste mixtures (Table 2), a smaller sub-set needs to be chosen for detailed studies.

Table 2. Mixture proportions for pastes evaluated in this study. All the pastes except HP-Control were proportioned using a (w/p)m of 0.20.

Mixture composition	Replacement material (% by mass of cement)			
	Fly Ash (F)/ Slag (S)	Metakaolin (K)	Microsilica (M)	Limestone (L); d_{50} of 1.5 or 3 µm[#]
UHP-control	0	0	0	0
HP-control	0	0	0	0
OPC + F/S	20, 30	0	0	0
OPC + M	0	0	10, 20	0
OPC + K	0	10	0	0
OPC + F/S + M	10, 20	0	10	0
OPC + F/S + K	10, 20	10	0	0
OPC + F/S + L	20	0	0	10a, 10b
OPC + F/S + L	25	0	0	5a, 5b
OPC + F/S + M + L	17.5	0	7.5	5b,5c
OPC + F/S + K + L	17.5	7.5	0	5b,5c

[#]The subscripts 'a', 'b' and 'c' along with the dosage of limestone powder indicate the type of limestone used in the mixture: 'a' – 1.5 µm limestone, 'b' – 3 µm limestone and 'c' – 50% 1.5 µm + 50% 3 µm limestone.

3.2 Microstructural Packing

Microstructural models were created for all the paste mixtures to analyze particle contacts and inter-particle interactions (Arora et al. 2018; Arora, Sant, and Neithalath 2016; Vance et al. 2015). The mean centroidal distance, coordination number and the number density are extracted from the analysis of the virtual RVEs. The mean centroidal distance is a measure of the packing density of the microstructure. It is calculated as the average distance to the center of a particle from the centroid of the microstructure. The coordination number is defined as the average number of nearest neighbor pairs in the microstructure. For any particle, the nearest neighbor is defined as a particle that lies either wholly or partially in the radial field of that particle, defined as a field with a radius of (r+5) µm, where 'r' is the radius of the particle. The number density is defined as the number of particles in a unit volume. It is directly related to the overall fineness of the powders in the paste.

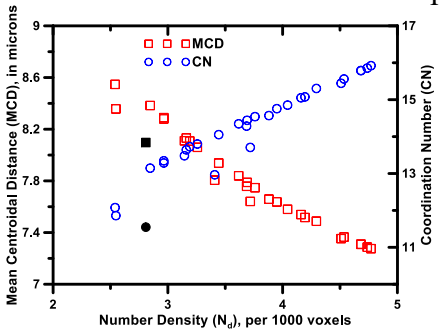

Figure 2. Relationships between the number density, mean centroidal distance and coordination number for the UHP pastes. The values for the UHP-control paste are shown using filled symbols.

Figure 2 shows that as the number density increases, the mean centroidal spacing between the particles decreases and the coordination number increases. The coordination number as well as the number density indicates the interparticle contacts in the microstructure and thus can be related to the yield stress of the paste and its degree of hydration at early ages. Moreover, plastic viscosity has been stated to be dependent heavily on the solid volume fraction (and thus the surface contacts) in the

paste, thereby relating to the above-mentioned parameters. These microstructural parameters can therefore be considered to influence both the rheology and hydration in cementitious materials.

3.3 Rheological Parameters

Rheological studies provide an understanding of the fresh state behavior of cementitious mixes and serve to monitor structure development that dictates the development of the mechanical properties. The yield stress, plastic viscosity and area of mini-slump (A_{ms}) were selected as the rheological parameters for this study. Figures 3(a) and (b) show these results. The areas of the mini-slump spread are shown by normalizing them with respect to the spread area for the UHP-control paste. The numbers as subscripts in the mixture labels indicate the OPC replacement level with that material.

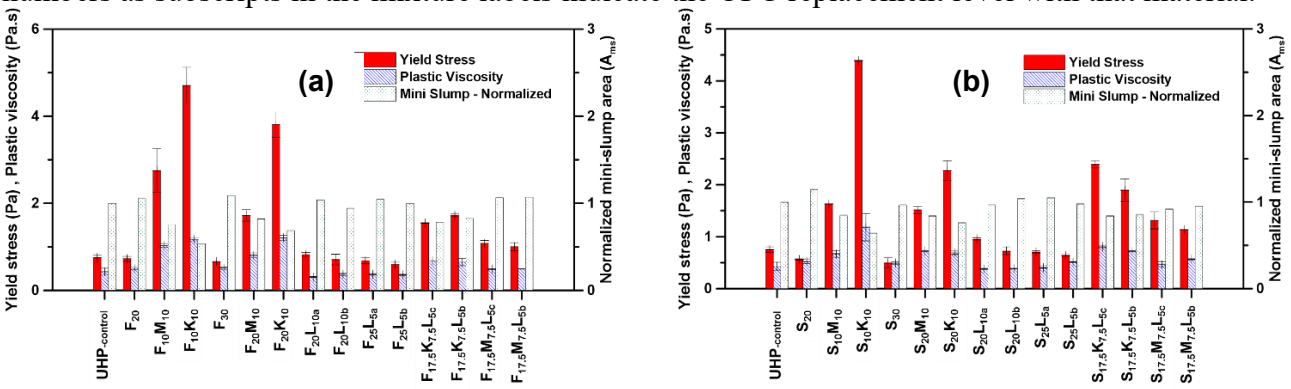

Figure 3. Yield stress, plastic viscosity and normalized mini slump values for pastes containing: (a) fly ash as the primary cement replacement material, and (b) slag as the primary cement replacement material.

It is observed from Figure 3 that the yield stress values are directly related to the plastic viscosity values for all the paste mixtures, even if not proportionally. The mini-slump values are inversely related to yield stress and plastic viscosity. Binary pastes containing fly ash or slag demonstrate relatively lower yield stress and plastic viscosity values as compared to the UHP-control paste. This is due to the lower inter-particle frictional forces in these pastes; a result of particle sizes and surface characteristics. It is also seen that the ternary mixes containing metakaolin show high yield stress values; however, incorporation of fine limestone reduces the yield stress in quaternary mixtures. The presence of fine limestone improves the overall packing and reduces the inter-particle friction (Vikan and Justnes 2007; Vance et al. 2013) in the quaternary mixtures thus lowering the yield stress and plastic viscosity, thereby leading to increased flowability of these mixtures.

3.4 Selection Criteria Based on Microstructural and Rheological Parameters

Figure 4 shows a schematic of the algorithm for binder selection based on the microstructural and rheological parameters. The third step in Figures 4(a) and (b) illustrates the selection criteria using these parameters individually, or their combinations (packing and flow coefficients) to select a smaller sub-set of binders from the ones shown in Table 2. The microstructural packing criteria are defined (Figure 4(a)) such that the selected binder demonstrates a higher degree of packing as compared to the control UHP binder, which is used as the baseline case. The flowability criteria are defined (Figure 4(b)) such that the selected binder has an acceptable workability as compared to the control UHP binder. Two strategies (Model 1 and Model 2) are presented for preliminary evaluation of the 31 binders in Table 2 to evaluate their suitability as UHP binders. Model 1 compares the individual microstructure and rheological parameters with the respective UHP parameters. It is obvious that a lower mean centroidal distance, a higher coordination number, and a higher number density will lead to a densely packed microstructure. Along with that, a workable mixture will have a lower yield stress and plastic viscosity and a higher mini-slump spread. Thus, the potential UHP binder should satisfy all the three rheology criteria. It should be noted here, however that the constants used as multipliers

for the UHP control parameters in Model 1 are user-defined constants and may be changed depending on the packing and workability requirements for the specific application.

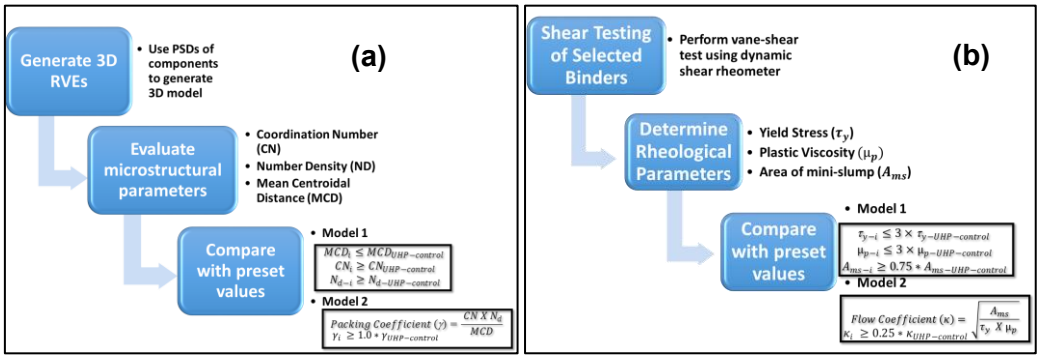

Figure 4. Binder selection strategy based on: (a) microstructural parameters, and (b) rheological parameters

Model 2 combines the rheological and microstructural parameters to calculate flow and packing coefficients of each preliminary mix design. The values for both these coefficients are normalized with respect to the control UHP binder. A higher value for γ indicates better packing whereas a higher value for κ indicates better workability for the UHP paste. Like the discussion above, the constant multipliers (1.0 for γ and 0.25 for κ) are user-defined and enable the user to have control over the selection of binder based on the desired application. Figure 5 shows the selected binders.

K_{10}	M_{10}	M_{20}	F_{20}	F_{30}	S_{20}	S_{30}	
$F_{10}K_{10}$	$F_{20}K_{10}$	$S_{10}K_{10}$	$S_{20}K_{10}$	$F_{10}M_{10}$	$F_{20}M_{10}$	$S_{10}M_{10}$	$S_{20}M_{10}$
$F_{20}L_{10a}$	$F_{20}L_{10b}$	$F_{25}L_{5a}$	$F_{25}L_{5c}$	$S_{20}L_{10a}$	$S_{20}L_{10b}$	$S_{25}L_{5a}$	$S_{25}L_{5b}$
$F_{17.5}K_{7.5}L_{5b}$	$F_{17.5}K_{7.5}L_{5c}$	$F_{17.5}M_{7.5}L_{5b}$	$F_{17.5}M_{7.5}L_{5c}$	$S_{17.5}K_{7.5}L_{5b}$	$S_{17.5}K_{7.5}L_{5c}$	$S_{17.5}M_{7.5}L_{5b}$	$S_{17.5}M_{7.5}L_{5c}$

Figure 5. Matrix of mixtures with the highlighted cells showing the mixtures selected based on packing and flow coefficients. Mixtures in the dark shaded cells were chosen for detailed studies

The selection of eight binders in Figure 5 was based on the relative chemical compositions and reactivity of the components. For instance, (i) only ternary and quaternary binders are considered because of their better packing, with limestone included only in the quaternary binders, (ii) a total cement replacement level of 30% is used to ensure sustainable UHP binders, (iii) limestone is considered only in binders containing metakaolin or microsilica since its size range is in between those of fly ash/slag and microsilica/metakaolin, and its low reactivity (Vance et al. 2013) limits the dosage to 5% (even though a recent study has shown increasing strengths with increasing limestone content in UHPC (W. Huang et al. 2017)), and (iv) when limestone is used, equal proportions of those with d_{50} values of 1.5 μm and 3 μm are preferred for improved packing.

3.5 Compressive Strength Development of Selected Binders

Compressive strength testing was carried out on 50 mm cubes cast for all the eight selected binders after 14 and 28 days of moist curing (Figure 6). The mass-based water to binder ratio was kept constant at 0.22 and the HRWR dosage was maintained at 1.25% (solids content). The volume fraction of paste in these mortars was kept at 50%. A regular high-performance plain cement mortar (w/c = 0.32) was also formulated for comparison. It is observed that even with a clinker factor reduction of 30%, most of the UHP mortars, especially the quaternary blends demonstrate 28-day strengths that are comparable to, or higher than that of the control UHP mortar. The mixtures containing slag demonstrate higher strengths than those containing fly ash at 28 days, but it is conceivable that the pozzolanic reaction of fly ash and its later synergy with the other replacement materials could improve the strength with further curing. It is noted that the addition of fibers,

reduction of water to binder ratio, optimization of the aggregate size fractions would lead to a final mixture with 28-day compressive strengths in excess of 150 MPa.

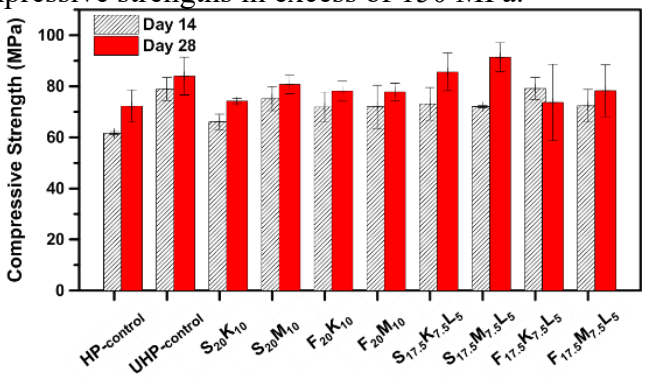

Figure 6. 14-day and 28-day compressive strengths of selected UHP mortars.

4. DESIGN OPTIMIZATION FOR CONCRETE

4.1 Particle Packing Based Design of UHPC

The mixture proportioning approach for UHPC must also ensure appropriate selection of the aggregate phases in addition to having the ideal paste phase. The selection of aggregates is governed by aggregate packing at the meso-scale since average aggregate sizes are about 100 times larger than the average sizes of the powders in the pastes. The use of a proper size distribution of aggregate particles can help increase the overall packing density of the concrete mixture in combination with the use of a properly chosen paste phase.

The current study uses a compressible packing model (Stovall, de Larrard, and Buil 1986) to calculate the packing density of a mixture consisting of different volume proportions of aggregates. The packing density Φ of the mixture is related to the compaction index K using equation 1. 'K' is a scalar index that depends on the physical process used for aggregate packing. 'K' value of 9 is used when a combination of vibration and compression is used to obtain the final aggregate mixture.

$$K = \sum_{i=1}^{n} \frac{y_i/\beta_i}{1/\Phi - 1/\gamma_i} \quad (1)$$

Here, y_i are the control parameters of the experiment and represent the individual volume fractions of the aggregates in the mixture. The residual packing density β_i represents the packing density of a mixture containing only the aggregate class 'i'. The values for residual packing density are determined experimentally using the dry rodded unit weight test. The virtual packing density γ_i is the theoretical value of packing density for the aggregate mixture when aggregate class 'i' is dominant. A dominant aggregate class is the one with the maximum volume fraction among all the other aggregate classes. Equation 1 is numerically solved using Newton-Raphson method to obtain the packing density Φ. The complete approach is detailed in (Arora 2018).

4.2 Aggregate Optimization – Results

For UHPC to be used in larger volumes such as in bridge decks and piers, the use of coarser particles needs to be considered to minimize volume changes and to reduce cost. The selection of appropriate aggregate gradation was done by optimizing the particle packing to obtain the maximum particle packing density in the known aggregate volume. Aggregate sizes as described in section 2.1 were used. The optimum fraction of individual aggregate classes required to achieve the maximum packing density was obtained by solving Equation 1 for multiple aggregate combinations. The volume fraction of each aggregate class was varied from 0.0 to 1.0 in increments of 0.1. This resulted in a total of 885 different aggregate combinations. A computer program was developed to automatically choose the aggregate combinations and input them into the algorithm for packing density determination. In Figure 7(a), the volume fraction of the coarse aggregate is the combined volume fraction of aggregates

whose nominal maximum size exceeds 2.36 mm, which are the 6.25 mm, 4.75 mm and 2.36 mm nominal maximum size aggregates. Similarly, in Figure 7(b), fine aggregate refers to the sands of median sizes 0.6 mm and 0.2 mm.

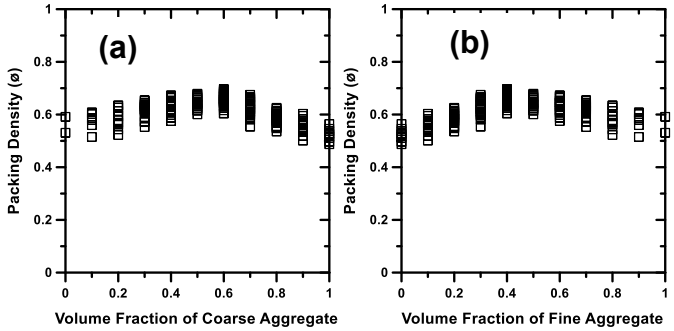

Figure 7. Packing density as a function of volume fractions of: (a) coarse aggregate, (b) fine aggregate

For each value of volume fraction of coarse aggregate (Figure 7(a)) on the x-axis, one can notice multiple values of the calculated packing density. These values correspond to the packing densities obtained by using different combinations of the chosen aggregates that result in a net coarse aggregate volume fraction equal to that shown on the x-axis. For instance, a coarse aggregate volume fraction of 0.60 may be achieved using multiple aggregate combinations of coarse aggregates (nominal maximum sizes of 6.25mm, 4.75mm, and 2.36 mm).

Maximum packing density occurs (Figure 7(a)) when the volume fraction of coarse aggregates is 60%. The plot of packing density as a function of aggregate size combinations helps understand the combined effect of coarse and fine aggregates on the packing density of the mixture. It is noted from Table 3 that the maximum value of packing fraction, ø is obtained as 0.696 for 40% fine aggregate, consisting of equal fractions of the 0.6 mm and the 0.2 mm sands, and 60% coarse aggregate, consisting of 40%, 10% and 10% fractions of 6.25 mm, 4.75 mm and 2.36 mm sized aggregates respectively. Such high degree of aggregate packing coupled with an optimized paste content is expected to lead to a dense concrete microstructure and subsequently result in lower porosity and higher strengths. Selected packing fraction values calculated were also verified using dry rodded unit weight testing. The aggregate combination with the highest packing fraction value was further selected for casting UHPC mixtures.

Table 3. Packing Fraction values for selected aggregate combinations.

6.25 mm	4.75 mm	2.36 mm	Sand (0.6 mm)	Sand (0.2 mm)	Packing Fraction
0.4	*0.1*	*0.1*	*0.2*	*0.2*	*0.696*
0.1	0.3	0.1	0.3	0.2	0.675
0.2	0.1	0.4	0.1	0.2	0.634
0	0	0	0.6	0.4	0.591
0.2	0.1	0.5	0.1	0.1	0.587
0.1	0.1	0.8	0	0	0.494

5. PROPERTIES OF SELECTED UHPC MIXTURES

5.1 Compression Strengths

Concrete cylinders were cast for two UHP binder designs (Table 4). Two concrete batches were prepared for each binder mixture, one with steel fibers (1%) and another without. It was found that the compressive strength (Figure 8) of all the specimens exceed 140 MPa at 28 days. The mixture containing fly ash, silica fume, and limestone, with an overall cement replacement level of 30%, was found to have the highest 28-day strength, of 153 MPa. The mixtures with fibers show comparable strengths as that of the mixtures without fibers, which is expected since 1% by volume of fibers do not contribute significantly to the compressive strength.

Table 4. – Mixture proportions for concrete mixtures. All the starting material contents, except the fiber content are relative masses with respect to that of the OPC.

Mixture components	$F_{17.5}M_{7.5}L_5$	$F_{17.5}M_{7.5}L_5$-f	$M_{20}L_{30}$	$M_{20}L_{30}$-f
OPC	1.0	1.0	1.0	1.0
Fly Ash (FA)	0.175	0.175	-	-
Silica Fume (SF)	0.075	0.075	0.20	0.20
Limestone (LS)	0.05	0.05	0.30	0.30
HRWR	0.0125	0.0125	0.0127	0.0127
Steel Fibers (% by volume)	-	1.0	-	1.0
w/b (mass-based)	0.165	0.168	0.180	0.185
Aggregate/Binder	0.7	0.7	0.7	0.7

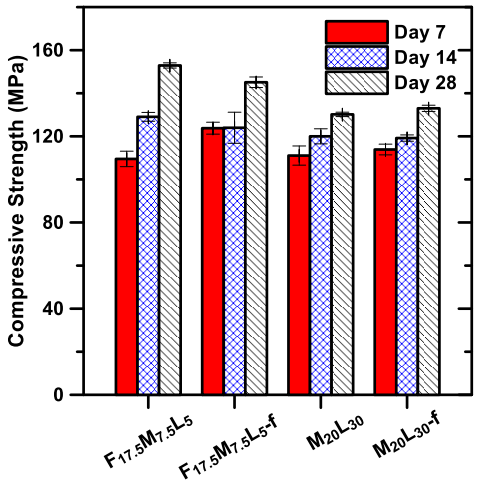

Figure 8. Compressive strength of UHPC mixtures after 7, 14 and 28 days of curing

6. CONCLUSIONS

This paper has described rational methodologies for the design of UHPCs derived from the fundamental understanding of paste phase at the microstructure level and aggregate phase at the mesostructure level. The ideal paste formulation suitable to exhibit ultra-high performance was selected from several binary, ternary, and quaternary blends using a stepwise algorithm that considered the effect of both microstructural packing as well as rheological properties of the binder. The proposed methodology allows the user to select mixtures based on acceptable ranges of microstructural packing and rheological parameters demanded by the application. In the next step, one quaternary binder containing fly ash, microsilica and limestone, and one ternary binder containing microsilica and limestone were identified for detailed studies. A compressible packing model was used for the packing of coarse and fine aggregates. A computer program analyzed 885 combinations of the three coarse and two fine aggregate sizes and arrived at the densest packing (of 0.696). Highly flowable concretes (due to the rheology of the paste formulation) were proportioned using the chosen aggregate combination and two of the selected binders. 28-day compressive strengths more than 150 MPa were obtained, validating the material design procedure.

7. ACKNOWLEDGEMENTS

The authors acknowledge the Arizona Department of Transportation (ADOT) for funding this research (Grant no: SPR 745). Materials were provided by BASF Corporation, Salt River Materials Group, Holcim Cement, Burgess Pigments, and Omya A.G.. This research was conducted in the Laboratory for the Science of Sustainable Infrastructural Materials at Arizona State University and the support that has made this laboratory possible is acknowledged. The contents of this paper reflect the views of the authors who are responsible for the facts and accuracy of the data presented herein, and do not necessarily reflect the views and policies of the funding agency, nor do the contents constitute a standard, specification, or a regulation.

8. REFERENCES

Arora, A., Aguayo, M., Mobasher, B., and Neithalath, N. n.d. "Microstructural Packing- and Rheology-Based Binder Selection and Characterization for Ultra-High Performance Concrete (UHPC) [Accepted for Publication]." *Cement and Concrete Research*.

Arora, Aashay. 2018. "Evaluation of the Performance of Multi-Component Cementitious Composites: Multi-Scale Experimental Characterization and Numerical Simulation." Ph.D., United States -- Arizona: Arizona State University. https://search.proquest.com/pqdtglobal/docview/2154864839/abstract/9B029C95683F4B09PQ/1.

Arora, Aashay, Matthew Aguayo, Hannah Hansen, Cesar Castro, Erin Federspiel, Barzin Mobasher, and Narayanan Neithalath. 2018. "Microstructural Packing- and Rheology-Based Binder Selection and Characterization for Ultra-High Performance Concrete (UHPC)." *Cement and Concrete Research* 103 (January): 179–90. https://doi.org/10.1016/j.cemconres.2017.10.013.

Arora, Aashay, Gaurav Sant, and Narayanan Neithalath. 2016. "Ternary Blends Containing Slag and Interground/Blended Limestone: Hydration, Strength, and Pore Structure." *Construction and Building Materials* 102, Part 1 (January): 113–24. https://doi.org/10.1016/j.conbuildmat.2015.10.179.

Burroughs, Jedadiah F., Jay Shannon, Todd S. Rushing, Kevin Yi, Quinn B. Gutierrez, and Danny W. Harrelson. 2017. "Potential of Finely Ground Limestone Powder to Benefit Ultra-High Performance Concrete Mixtures." *Construction and Building Materials* 141 (June): 335–42. https://doi.org/10.1016/j.conbuildmat.2017.02.073.

De Larrard, Francois. 1999. *Concrete Mixture Proportioning: A Scientific Approach*. CRC Press.

Ghafari, Ehsan, Mahdi Arezoumandi, Hugo Costa, and Eduardo Júlio. 2015. "Influence of Nano-Silica Addition on Durability of UHPC." *Construction and Building Materials* 94 (September): 181–88. https://doi.org/10.1016/j.conbuildmat.2015.07.009.

Ghafari, Ehsan, Hugo Costa, Eduardo Júlio, António Portugal, and Luisa Durães. 2014. "The Effect of Nanosilica Addition on Flowability, Strength and Transport Properties of Ultra High Performance Concrete." *Materials & Design* 59 (July): 1–9. https://doi.org/10.1016/j.matdes.2014.02.051.

Graybeal, B. 2011. "FHWA TECHNOTE: Ultra High Performance Concrete." *FHWA Publication No: FHWA-HRT-11-038: Federal Highway Administration*.

Graybeal, Benjamin A. 2012. *Ultra-High Performance Concrete Composite Connections for Precast Concrete Bridge Decks*. US Department of Transportation, Federal Highway Administration.

Huang, Huanghuang, Xiaojian Gao, Hui Wang, and Huan Ye. 2017. "Influence of Rice Husk Ash on Strength and Permeability of Ultra-High Performance Concrete." *Construction and Building Materials* 149 (Supplement C): 621–28. https://doi.org/10.1016/j.conbuildmat.2017.05.155.

Huang, Wei, Hadi Kazemi-Kamyab, Wei Sun, and Karen Scrivener. 2017. "Effect of Cement Substitution by Limestone on the Hydration and Microstructural Development of Ultra-High Performance Concrete (UHPC)." *Cement and Concrete Composites* 77 (March): 86–101. https://doi.org/10.1016/j.cemconcomp.2016.12.009.

Le Hoang, An, and Ekkehard Fehling. 2017. "Influence of Steel Fiber Content and Aspect Ratio on the Uniaxial Tensile and Compressive Behavior of Ultra High Performance Concrete." *Construction and Building Materials* 153 (Supplement C): 790–806. https://doi.org/10.1016/j.conbuildmat.2017.07.130.

Li, Wengui, Zhengyu Huang, Fangliang Cao, Zhihui Sun, and Surendra P. Shah. 2015. "Effects of Nano-Silica and Nano-Limestone on Flowability and Mechanical Properties of Ultra-High-Performance Concrete Matrix." *Construction and Building Materials* 95 (October): 366–74. https://doi.org/10.1016/j.conbuildmat.2015.05.137.

Li, Zhengqi, Harish Kizhakkumodom Venkata, and Prasada Rao Rangaraju. 2015. "Influence of Silica Flour–Silica Fume Combination on the Properties of High Performance Cementitious Mixtures at Ambient Temperature Curing." *Construction and Building Materials* 100 (Supplement C): 225–33. https://doi.org/10.1016/j.conbuildmat.2015.09.042.

Maya, L. F., and B. Graybeal. 2017. “Experimental Study of Strand Splice Connections in UHPC for Continuous Precast Prestressed Concrete Bridges.” *Engineering Structures* 133 (Supplement C): 81–90. https://doi.org/10.1016/j.engstruct.2016.12.018.

Muhd Norhasri, M. S., M. S. Hamidah, A. Mohd Fadzil, and O. Megawati. 2016. “Inclusion of Nano Metakaolin as Additive in Ultra High Performance Concrete (UHPC).” *Construction and Building Materials* 127 (November): 167–75. https://doi.org/10.1016/j.conbuildmat.2016.09.127.

Reda, M. M, N. G Shrive, and J. E Gillott. 1999. “Microstructural Investigation of Innovative UHPC.” *Cement and Concrete Research* 29 (3): 323–29. https://doi.org/10.1016/S0008-8846(98)00225-7.

Roquier, G. 2016. “The 4-Parameter Compressible Packing Model (CPM) Including a New Theory about Wall Effect and Loosening Effect for Spheres.” *Powder Technology* 302 (Supplement C): 247–53. https://doi.org/10.1016/j.powtec.2016.08.031.

Russell, Henry G., and Benjamin A. Graybeal. 2013. “Ultra-High Performance Concrete: A State-of-the-Art Report for the Bridge Community.”

Shafieifar, Mohamadreza, Mahsa Farzad, and Atorod Azizinamini. 2017. “Experimental and Numerical Study on Mechanical Properties of Ultra High Performance Concrete (UHPC).” *Construction and Building Materials* 156 (Supplement C): 402–11. https://doi.org/10.1016/j.conbuildmat.2017.08.170.

Stovall, T., F. de Larrard, and M. Buil. 1986. “Linear Packing Density Model of Grain Mixtures.” *Powder Technology* 48 (1): 1–12. https://doi.org/10.1016/0032-5910(86)80058-4.

Tazarv, Mostafa, and M. Saiid Saiidi. 2015. “UHPC-Filled Duct Connections for Accelerated Bridge Construction of RC Columns in High Seismic Zones.” *Engineering Structures* 99 (Supplement C): 413–22. https://doi.org/10.1016/j.engstruct.2015.05.018.

Van Tuan, Nguyen, Guang Ye, Klaas van Breugel, and Oguzhan Copuroglu. 2011. “Hydration and Microstructure of Ultra High Performance Concrete Incorporating Rice Husk Ash.” *Cement and Concrete Research* 41 (11): 1104–11. https://doi.org/10.1016/j.cemconres.2011.06.009.

Vance, Kirk, Matthew Aguayo, Tandre Oey, Gaurav Sant, and Narayanan Neithalath. 2013. “Hydration and Strength Development in Ternary Portland Cement Blends Containing Limestone and Fly Ash or Metakaolin.” *Cement and Concrete Composites* 39 (May): 93–103. https://doi.org/10.1016/j.cemconcomp.2013.03.028.

Vance, Kirk, Aashay Arora, Gaurav Sant, and Narayanan Neithalath. 2015. “Rheological Evaluations of Interground and Blended Cement–Limestone Suspensions.” *Construction and Building Materials* 79 (March): 65–72. https://doi.org/10.1016/j.conbuildmat.2014.12.054.

Vikan, Hedda, and Harald Justnes. 2007. “Rheology of Cementitious Paste with Silica Fume or Limestone.” *Cement and Concrete Research* 37 (11): 1512–17. https://doi.org/10.1016/j.cemconres.2007.08.012.

Vítek, Jan L., Robert Coufal, and David Čítek. 2013. “UHPC – Development and Testing on Structural Elements.” *Procedia Engineering*, CONCRETE AND CONCRETE STRUCTURES 2013 - 6th International Conference, Slovakia, 65 (Supplement C): 218–23. https://doi.org/10.1016/j.proeng.2013.09.033.

Wang, Chong, Changhui Yang, Fang Liu, Chaojun Wan, and Xincheng Pu. 2012. “Preparation of Ultra-High Performance Concrete with Common Technology and Materials.” *Cement & Concrete Composites* 34 (4): 538–44. https://doi.org/10.1016/j.cemconcomp.2011.11.005.

Wille, Kay, and Christopher Boisvert-Cotulio. 2015. “Material Efficiency in the Design of Ultra-High Performance Concrete.” *Construction and Building Materials* 86 (July): 33–43. https://doi.org/10.1016/j.conbuildmat.2015.03.087.

Yoo, Doo-Yeol, and Nemkumar Banthia. 2016. “Mechanical Properties of Ultra-High-Performance Fiber-Reinforced Concrete: A Review.” *Cement and Concrete Composites* 73 (October): 267–80. https://doi.org/10.1016/j.cemconcomp.2016.08.001.